



# Development of a Ni/Al<sub>2</sub>O<sub>3</sub> Cermet-Supported Tubular Solid Oxide Fuel Cell Assembled with Different Functional Layers by Atmospheric Plasma-Spraying

Cheng-Xin Li, Chang-Jiu Li, and Guan-Jun Yang

(Submitted September 19, 2007; in revised form November 24, 2008)

A cermet-supported tubular configuration amenable to preparation by a relatively low-cost thermal spraying process is proposed. An Al<sub>2</sub>O<sub>3</sub>-Ni cermet thick deposit prepared by flame spraying is employed as both support tube and anode current collector. Atmospheric plasma spraying (APS) has been employed to prepare the anode, cathode, and stabilized ZrO<sub>2</sub>-based electrolyte with the aim of reducing manufacturing costs. Gas-tightness of the APS electrolyte has been achieved by a postdensification process. The effects of the densification process on the gas-tightness of the plasma-sprayed YSZ electrolyte and the open-circuit voltage of the SOFC have been investigated. The effects of the microstructures of the plasma-sprayed anode, electrolyte, and cathode on the performance of the SOFC test cell have been investigated.

**Keywords** cermet, flame spraying, plasma spraying, solid oxide fuel cell, stabilized zirconia

## 1. Introduction

Solid oxide fuel cells (SOFCs) combine the benefits of environmentally benign power generation with fuel flexibility. Their reliable operation as high power generation systems at high temperatures can be obtained with a tubular design. To date, stationary SOFC units providing powers in the range 1-500 kW have been successfully manufactured for demonstration. Net electrical efficiencies of up to 50% (Ref 1) and overall efficiencies of about 70-90% have been achieved (Ref 2). However, reduction of manufacturing costs is the biggest challenge for industrial commercialization of SOFCs (Ref 3).

Atmospheric plasma spraying (APS) is regarded as one of the most promising methods for manufacturing the components employed in SOFCs, which comprise a porous ceramic cathode and cermet anode, a dense ceramic electrolyte layer, and an interconnector, because of its fast deposition rate and cost-effective characteristics. Thermally sprayed ceramic deposits are characterized by a

porous and lamellar structure (Ref 4). A porous fraction ranging from a few % up to 20% can be obtained in a thermally sprayed ceramic coating (Ref 5). Pores in a coating will influence many of its properties, such as its mechanical and physical properties and its overall performance (Ref 4, 5). Pores in the coatings consist of relatively large voids ranging in size from several micrometers to several tens of micrometers and small two-dimensional voids such as the inter-lamellar nonbonded interfaces and vertical cracks in individual lamellae. Pores are therefore interconnected through vertical microcracks in individual splats in the coating (Ref 6), which permit the passage of gas through the coating. This allows thermally sprayed coatings to be employed as porous electrodes in SOFCs. As a result, APS has been employed to fabricate SOFC anodes (Ref 7) and cathodes (Ref 8). Moreover, it has also been employed to deposit interconnectors (Ref 9). However, APS YSZ coatings produced by the conventional route are generally not suitable for use as electrolytes in SOFCs due to their high gas permeability.

With a view to employing APS YSZ as an electrolyte for SOFCs, postspray treatments of the as-sprayed ceramic layer, such as sintering (Ref 10, 11) and infiltrating densification (Ref 12-14), have been attempted. Our previous studies have shown that through impregnation treatment at low temperature, APS YSZ coating can be densified to a gas permeability level satisfactory for the operation of SOFCs (Ref 12, 13). Therefore, APS YSZ coatings can be applied as the electrolytes in SOFCs after subjecting them to a postspray densification process.

In the work described herein, a Ni-YSZ anode, a perovskite ceramic cathode, and a YSZ electrolyte have been deposited by APS, and the influence of their

Cheng-Xin Li, Chang-Jiu Li, and Guan-Jun Yang, State Key Laboratory for Mechanical Behavior of Materials, School of Materials Science and Engineering, Xi'an Jiaotong University, Xi'an, Shaanxi 710049, P.R. China. Contact e-mail: licx@mail.xjtu.edu.cn.

microstructure on the performance of the SOFC has been examined. The performance was tested using a Ni-Al<sub>2</sub>O<sub>3</sub> cermet-supported tubular SOFC design. This configuration was adopted to combine the advantages of conventional tubular SOFCs with the high power density characteristics of planar SOFCs (Ref 12). Another characteristic of this design is that the electrodes and the electrolyte can be easily manufactured by thermal spraying. The cermet support in the SOFC cell also serves to collect current from the anode. The composition of the cermet can be adjusted to optimize the thermal expansion coefficient of the support and to match it with those of the other components.

## 2. Materials and Fabrication Processes

### 2.1 Ni-Al<sub>2</sub>O<sub>3</sub> Cermet Support

A free-standing Ni-Al<sub>2</sub>O<sub>3</sub> tube about 450 mm long was fabricated by oxygen-acetylene flame spraying (HP-2000, Xinye, Shanghai) using a powder blend of Ni-25 wt.% Al<sub>2</sub>O<sub>3</sub> (nickel-coated alumina powder) and NiO-50 wt.% Al<sub>2</sub>O<sub>3</sub> agglomerate. The weight ratio of Ni-25 wt.% Al<sub>2</sub>O<sub>3</sub> and NiO-50 wt.% Al<sub>2</sub>O<sub>3</sub> in the blended powder was 50:50. The NiO-50 wt.% Al<sub>2</sub>O<sub>3</sub> agglomerate was made of NiO and Al<sub>2</sub>O<sub>3</sub>, both of which had a particle size of <5 μm. Oxygen and acetylene were set at 0.5 and 0.1 MPa, respectively. The flow of oxygen was 1 L/min and the flow of acetylene was 2 L/min. The spray distance was 60 mm. The tube was prepared by flame-spraying on an aluminum support to a desired thickness, and then the Al supporting tube was removed by alkaline dissolution.

### 2.2 Anode (Fuel Electrode)

Spray powders for the anode were agglomerated with NiO of particle size <5 μm and YSZ (4.5 mol% Y<sub>2</sub>O<sub>3</sub>) of particle size <10 μm. The agglomerated powders had a particle size of <37.5 μm. For comparison, two powder mixtures, consisting of YSZ/NiO and Al<sub>2</sub>O<sub>3</sub>/NiO, were also employed.

### 2.3 Electrolyte

Two types of zirconia-based oxygen ion conductors were employed as electrolytes in the SOFCs, since they possess adequate oxygen ion conductivity and exhibit desirable chemical stability in both oxidizing and reducing atmospheres. One was a commercially available powder consisting of ZrO<sub>2</sub> stabilized by 8 mol% Y<sub>2</sub>O<sub>3</sub> (YSZ, 10-45 μm, Fujimi, Japan). The other powder, ZrO<sub>2</sub> stabilized by 10 mol% Sc<sub>2</sub>O<sub>3</sub> (ScSZ), was prepared by solid-phase reaction and sintering processes. After mixing Sc<sub>2</sub>O<sub>3</sub> and ZrO<sub>2</sub> in a molar ratio of 10:90 with the addition of 0.5% Al<sub>2</sub>O<sub>3</sub>, the mixture was ball-milled for 24 h using a YSZ cylinder and YSZ balls. The milled powder was calcined at 900 °C for 10 h and then sintered at 1450 °C for 10 h. The sintered powder was crushed and sifted to an appropriate particle size range for plasma spraying.

### 2.4 Cathode (Air Electrode)

Lanthanum strontium manganate (LSM) perovskite oxide was adopted as the cathode material due to its high electrical conductivity, good chemical compatibility with the stabilized ZrO<sub>2</sub> electrolyte, and an acceptable thermal compatibility with the other components in the SOFCs under the conditions of operation (Ref 15, 16). LSM of chemical formula La<sub>0.8</sub>Sr<sub>0.2</sub>MnO<sub>3</sub> was prepared by a conventional solid-phase sintering process by heating a stoichiometric mixture of La<sub>2</sub>O<sub>3</sub>, SrCO<sub>3</sub>, and MnCO<sub>3</sub> at 1200 °C for 24 h in air. The sintered powder was crushed and sifted to a suitable size range for plasma spraying.

### 2.5 Cell Fabrication

Table 1 shows the materials and processing methods used to obtain the different components of the test SOFC cell. A porous Ni-Al<sub>2</sub>O<sub>3</sub> cermet tube with a blind end and a thickness of 800 μm was produced by flame spraying. This supporting tube also served as the anode current collector. A Ni/YSZ anode layer with a thickness of 25 μm was deposited on the support tube by APS. Then, ZrO<sub>2</sub> electrolyte layers of different thicknesses were deposited on the anode layer by APS. The APS YSZ electrolyte layer was densified by impregnating the coating with yttrium/zirconium nitrate solution followed by heat-treatment at 400 °C (Ref 13), while the APS ScSZ electrolyte layer was densified by impregnating it with scandium/zirconium nitrate solution. YSZ and ScSZ deposits, both of which had been impregnated in 10 steps, were employed as the electrolytes of the test cells. The heat-treatment was conducted after each impregnation step. Finally, a LSM cathode layer of thickness 20 μm was deposited on the densified YSZ layer to construct the single test cell. The effective area of the single test cell was equal to the cathode surface area, which was set at 2 cm<sup>2</sup>.

Atmospheric plasma spraying was performed with a commercial plasma spraying system (Model GDP-80, 80 kW class, Jiujiang, China) using Ar-H<sub>2</sub> plasma. The anode and electrolyte were deposited at a power of 38.5 kW and a spray distance of 100 mm. The LSM cathode was deposited at a plasma power of 30 kW and a spray distance of 100 mm (Ref 17).

### 2.6 Cell Performance Test

A schematic diagram of the configuration of the single cell for the performance test is shown in Fig. 1. The

**Table 1** Materials and processing methods

	Anode	Electrolyte	Cathode
Materials	Ni/YSZ	YSZ or ScSZ	LSM
Voltage	55 V	55 V	50 V
Current	700 A	700 A	600 A
Primary gas (Ar)		0.7 MPa, 47.1 L/min	
Auxiliary gas (H <sub>2</sub> )	0.4 MPa, 12.5 L/min	0.4 MPa, 12.5 L/min	0.4 MPa, 5.6 L/min
Spray distance	100 mm	100 mm	100 mm
Thickness	25 μm	40-100 μm	20 μm

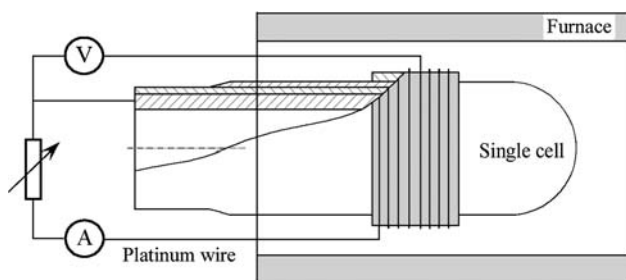


**Fig. 1** The configuration of the cell performance test

performance of the single cell was tested in a furnace with a heating/cooling rate of 3 °C/min. The open end of the tube extended to the outside of the furnace. Hydrogen as a fuel was bubbled through water maintained at about 30 °C. Pure oxygen was used in the cathode. The effective cathode area of the cell was 2.0 cm<sup>2</sup>. Platinum wire was wound around the cathode layer to collect current. The interval between two adjacent platinum wires was 0.5 mm. The performance of the cell was tested at different operating temperatures.

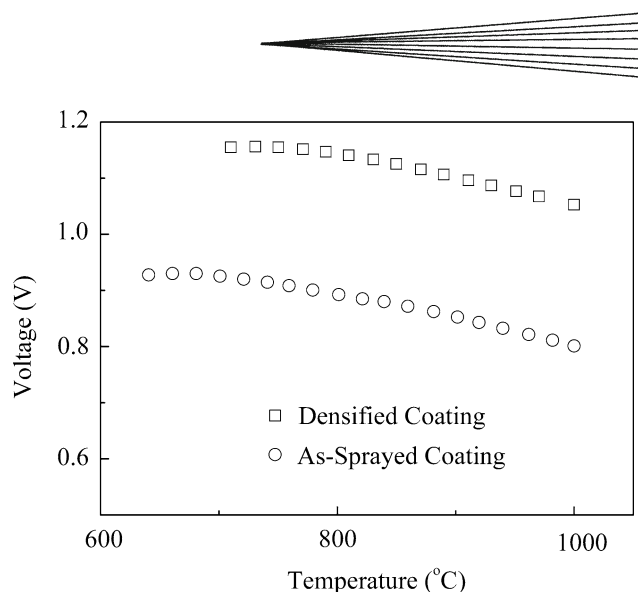
### 3. Results and Discussion

#### 3.1 Effect of Densification Treatment on the Gas Permeability of APS YSZ and the Open-Circuit Voltage of the Single Cell

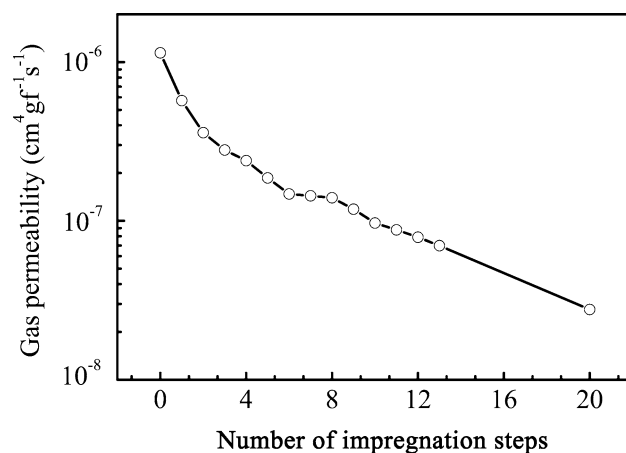
Figure 2 shows the change of the open-circuit voltage (OCV) with test temperature for a SOFC cell assembled using the as-sprayed YSZ with a thickness of 100 μm as the electrolyte. The OCV was measured using oxygen and hydrogen gases. The maximum OCV of the cell assembled with the as-deposited YSZ was about 0.93 V at a temperature of 600 °C. Due to high gas permeability resulting from the porous nature of the as-sprayed YSZ, which is an inherent feature of the thermal spray process, the OCV is significantly lower than the theoretical value. To reduce the gas permeability, APS YSZ was densified by infiltration of a nitrate solution into the deposit followed by heat treatment at 400 °C. The void network formed through inter-connecting of vertical cracks in splats with the non-bonded interface areas provides paths for the solution to fill the voids. Nano-YSZ particles formed through the decomposition of the infiltrated nitrate within the YSZ during heat-treatment fill-in all of the voids, including nonbonded interfaces and vertical cracks (Ref 18).

Figure 3 shows the effect of impregnation steps on the gas permeability of the cell. The gas permeability through the cell decreased with increasing number of impregnation steps. It can be seen that the gas permeability of the electrolytic layer was reduced from  $1.1 \times 10^{-6} \text{ cm}^4 \text{ gf}^{-1} \text{ s}^{-1}$  for the as-sprayed YSZ to about  $1.9 \times 10^{-7} \text{ cm}^4 \text{ gf}^{-1} \text{ s}^{-1}$  after 5 impregnation steps, and was further reduced to  $7.9 \times 10^{-8} \text{ cm}^4 \text{ gf}^{-1} \text{ s}^{-1}$  after 12 steps (Ref 19).

Tsukuda et al. (Ref 20) reported the performance of a 10 kW class SOFC module. In their module, the YSZ



**Fig. 2** Effect of impregnating treatment on the OCV of the test cell



**Fig. 3** Effect of impregnation steps on the gas permeability of the APS YSZ coating

electrolyte was deposited by vacuum plasma spraying (VPS). The gas permeability of the electrolyte layer deposited by VPS was about  $6.0 \times 10^{-7} \text{ cm}^4 \text{ gf}^{-1} \text{ s}^{-1}$ . It is clear that after five infiltration treatments the gas permeability of APS YSZ becomes lower than that of VPS YSZ, which has found practical application in a SOFC module displaying long-term operation up to 2000 h. Therefore, the densified APS YSZ layer should be applicable as the electrolyte of SOFCs.

It can also be seen in Fig. 2 that the maximum OCV of the cell assembled with the densified APS YSZ reached 1.16 V at 700 °C and 1.10 V at 900 °C. These values are approximately equal to the theoretical value for a cell assembled with dense YSZ material.

Although the APS method has been adopted to fabricate the anode and cathode of a SOFC because of its cost-effectiveness, the as-sprayed YSZ coating cannot be directly used as an electrolyte because of its high porosity.

The as-sprayed coating is usually sintered at a temperature in excess of 1200 °C in order to utilize the cost-effective method. However, a high sintering temperature will increase the cost of SOFC fabrication and may also lead to the reaction of YSZ with other layers. The postspray impregnation densification treatment of APS electrolyte at 400 °C is effective to reduce the gas permeability and subsequently the densified APS electrolyte can fulfill the requirement of gas-tightness of SOFC electrolyte. Moreover, compared with the as-sprayed coatings, the electrical conductivity was improved by about 20-25% through the densification treatment (Ref 13).

### 3.2 Effect of the Composition and Structure of the Anode on the Performance of the Cell

Ni/YSZ composite is widely used as the anode material in high-temperature SOFCs due to its excellent catalytic properties, high thermal stability, and fairly low cost. The polarization characteristics of the anode are highly dependent on its microstructure. It is considered that the anode activity can be improved through increasing the triple-phase boundaries (TPBs) at the electrolyte/anode interface. The active TPB length, and consequently the performance of the cell, can be adjusted by varying the composition and microstructure of the APS anode through appropriate manipulation of feedstocks. Table 2 shows the compositions of three different types of anodes that were used to investigate the effect of anode composition on the performance of the cell. The feedstocks for Anode A and Anode B were composed of large Ni and ceramic particles, and the two powders were mechanically mixed to obtain the starting composite powders for deposition of the anodes. The ceramic composition in the composite anode provides the anode with a resistance to sintering during prolonged high-temperature operation. Moreover, the YSZ in the composite anode may extend the TPB into the anode layer and increase the TPB length. To improve the uniformity of the distribution of Ni and YSZ particles, the spray powder for Anode C was prepared by agglomeration of small NiO and YSZ particles. NiO is reduced to active Ni under hydrogen atmosphere prior to SOFC operation.

Figure 4 shows the test results of the performances of the cells with different anodes. The cell assembled with the type A anode exhibited a maximum power density of 0.15 W/cm<sup>2</sup> at 1000 °C because of limited active TPB at the interface between the electrolyte and the anode. It can

**Table 2** Nominal compositions and manufacturing processes of anode feedstocks

Type	Compositions	Material method	Particle size, $\mu\text{m}$
Anode A	Ni (<50 $\mu\text{m}$ ) + Al <sub>2</sub> O <sub>3</sub> (10-40 $\mu\text{m}$ )	Mechanical blend	10-50
Anode B	Ni (<50 $\mu\text{m}$ ) + YSZ (10-45 $\mu\text{m}$ )	Mechanical blend	10-50
Anode C	NiO (<5 $\mu\text{m}$ ) + YSZ (<10 $\mu\text{m}$ )	Agglomerated	<37.5

clearly be observed that when the ceramic constituent in the composite anode is changed from insulating Al<sub>2</sub>O<sub>3</sub> to the electrolyte material YSZ, the polarization of the cell is remarkably reduced and the maximum output power density increases to about 0.4 W/cm<sup>2</sup> at 1000 °C with the type B anode. This is due to the fact that the substitution of Al<sub>2</sub>O<sub>3</sub> by YSZ extends active TPBs from the interface between the electrolyte and anode into the anode. Moreover, it was found that the cell assembled with the type C anode exhibited a maximum power density of 0.58 W/cm<sup>2</sup> at 1000 °C at a current density of 1.2 A/cm<sup>2</sup>. These results clearly indicate that APS Ni/YSZ is an active anode material for high-temperature operation of SOFCs. Moreover, the cell performance is significantly influenced by the microstructure of the APS anode. Therefore, the present results indicate that the active TPBs can be further increased through appropriate design of the APS feedstock for the SOFC anode.

From the results shown in Fig. 4, it can also be seen that the cell voltage decreased linearly with increasing current density when the current density was larger than about 0.2 A/cm<sup>2</sup>. This means that the output performance of the present cells is controlled by ohmic polarization at high output current density levels. Moreover, concentration polarization was not observed, even at current densities of up to 1.2 A/cm<sup>2</sup>. This result indicates that the cermet support deposited by flame spraying and the anode deposited by APS have enough through-thickness pores to permit transport of the reacting gas to the active TPB zone of the anode.

### 3.3 Effect of Electrolyte Ohmic Losses

Stabilized zirconia is the most commonly used electrolyte material for SOFCs because of its unique properties, such as high chemical and thermal stability and pure ionic conductivity over a wide range of conditions. However, the electrical conductivity of a stabilized zirconia electrolyte is three orders of magnitude lower than those of anode and cathode materials. The electrical

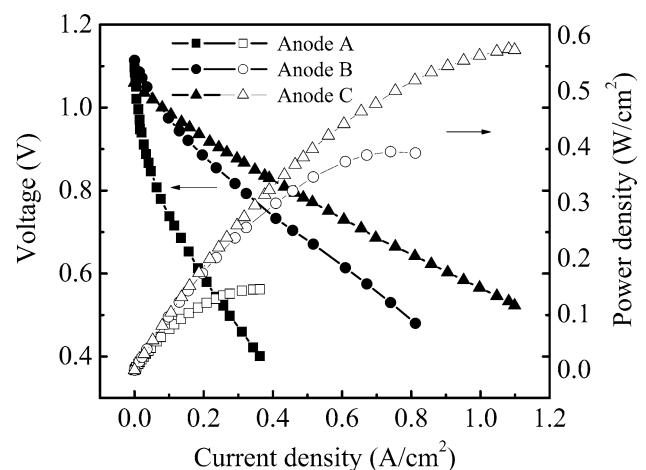


**Fig. 4** Cell performance with different anode compositions at a temperature of 1000 °C

conductivity of the plasma-sprayed YSZ was furthermore less than one-third of that of the bulk material (Ref 13). Therefore, the ohmic loss of the electrolyte may dominate the performance of SOFCs assembled with APS electrolyte. Many scientists and researchers have dedicated their efforts to the development of thin YSZ deposition technology, applying many processing methods, with a view to reducing the ohmic loss by the reduction of electrolyte thickness (Ref 21). Plasma spraying is practically employed to deposit thick coatings. Recently, attempts have been made to deposit a thin ceramic coating by plasma spraying to fulfill the requirements of a thin solid electrode for SOFC operation (Ref 22-24). Henne et al. (Ref 22, 23) showed that a SOFC assembled with vacuum plasma-sprayed YSZ with a thickness of about 30  $\mu\text{m}$  exhibited high-output performance. Our previous study (Ref 25) showed that the thickness of APS YSZ significantly influences the performances of SOFCs through ohmic polarization. Therefore, the effect of YSZ ohmic loss on the performance of SOFCs was examined using cermet-supported tubular SOFCs assembled with APS YSZ of different thicknesses and APS ScSZ.

After the type C anode had been deposited on the Ni/Al<sub>2</sub>O<sub>3</sub> cermet tube used for the test, YSZ layers of three different thicknesses were deposited on the anode in a stepwise fashion. The YSZ layer thicknesses were 40, 75, and 100  $\mu\text{m}$ , respectively. They were densified through the impregnation process mentioned previously (Ref 13). An LSM cathode layer of thickness 20  $\mu\text{m}$  was deposited on the densified YSZ layer to assemble a SOFC single cell.

Figure 5 shows the power generation characteristics of the cermet-supported tubular SOFC single cell with different YSZ electrolyte thicknesses at 900 °C. It was found that the reduction of YSZ thickness led to an increase in the SOFC performance despite a reduction in the OCV. For an electrolyte thickness of 100  $\mu\text{m}$ , the maximum power density reached 0.28 and 0.47 W/cm<sup>2</sup> at 900 °C and 1000 °C, respectively (Ref 25).

Concentration polarization did not occur, even when the current density reached about 1.2 A/cm<sup>2</sup>. This result

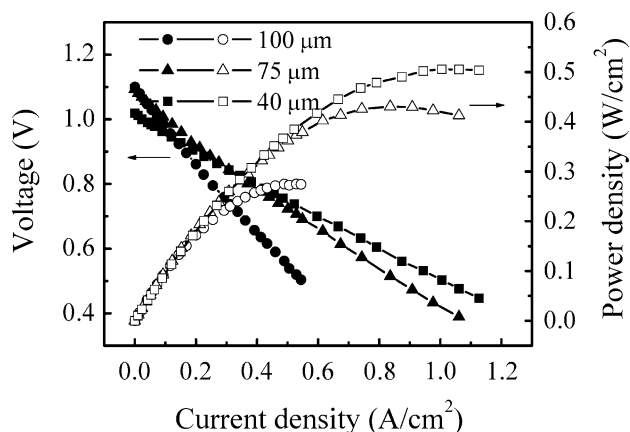


**Fig. 5** Performance of the cell with different YSZ electrolyte thicknesses at 900 °C

indicated that the cermet support deposited by flame spraying and the anode and LSM cathode deposited by APS have enough through-thickness pores to permit diffusion of the reacting gas to the active TPB zone of the electrodes. When the YSZ thickness was decreased to 40  $\mu\text{m}$ , the maximum power density increased to 0.51 and 0.76 W/cm<sup>2</sup> at 900 and 1000 °C, respectively. Using APS YSZ of thickness 75  $\mu\text{m}$ , the maximum power densities were 0.43 and 0.64 W/cm<sup>2</sup> at 900 and 1000 °C, respectively.

Since the electrical conductivity of the YSZ electrolyte is lower than those of the other component materials, the reduction of the electrolyte resistance achieved by reducing the YSZ layer thickness leads to a substantial reduction of the ohmic polarization. On reducing the electrolyte thickness from 100 to 40  $\mu\text{m}$ , the maximum output power density at 900 and 1000 °C increased by about 82% and 62%, respectively. A further reduction of the electrolyte resistance can be realized by substituting YSZ with ScSZ, which has high ionic conductivity (Ref 26).

Figure 6 shows the influence of electrolytic materials on the maximum output power density of SOFC single cells assembled with the APS electrolyte at a thickness of 40  $\mu\text{m}$  at different temperatures. The effect of temperature on the maximum output power density of the cell with the ScSZ electrolyte is similar to that seen for the cell with the YSZ electrolyte. This is because the electrical conductivity of doped zirconia electrolyte increases with increasing temperature. The maximum output power density reached 0.89 W/cm<sup>2</sup> with the high electrical conductivity of ScSZ electrolyte of thickness 40  $\mu\text{m}$  at 1000 °C. The maximum output power density of the cell incorporating ScSZ was clearly higher than that of the cell incorporating YSZ.

Reducing the ohmic loss of the electrolyte layer through reducing the electrolyte thickness, increasing the operation temperature, and increasing the electrical conductivity of the electrolyte obviously improved the

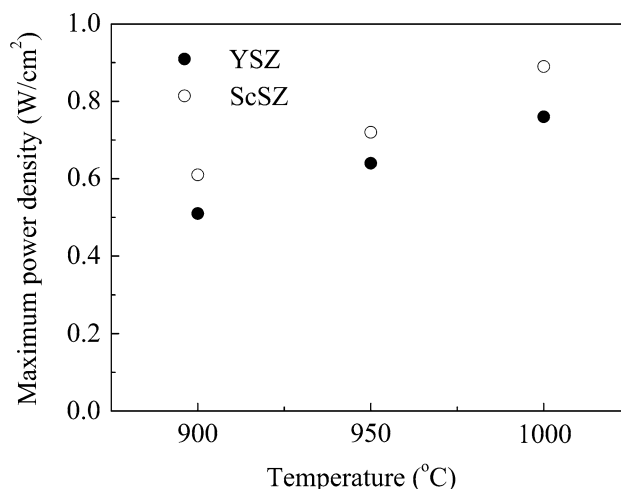


**Fig. 6** Performance of SOFC single cells with different electrolytic materials

SOFC performance. However, although the ionic conductivity of ScSZ bulk material is twice that of YSZ, the improvement in the cell's performance in terms of the maximum output power density was only about 17%. This further highlights the importance of optimizing the electrodes in the SOFCs with the thin ZrO<sub>2</sub>-based electrolyte. In our previous study, we established that when the maximum output power density is increased beyond a certain level, the output power density of the cell becomes controlled by the electrode polarization, which is dominated by the number of active TPBs between the electrode and electrolyte (Ref 25). Therefore, it is necessary to design and create more effective TPBs between the electrode and electrolyte to achieve a further significant improvement in the output performance of the present plasma-sprayed tubular SOFCs.

### 3.4 Effect of APS Cathode Thickness on the Cell Performance

Plasma-sprayed LSM was considered as a suitable cathode material for SOFCs due to its porous microstructure. However, a high-performance cathode requires appropriate porosity and high electrical conductivity. Moreover, the thickness of the APS LSM layer may also affect the output performance of the SOFC because the connected porosity of a plasma-sprayed ceramic coating decreases remarkably with increasing coating thickness (Ref 6, 27).

Three cells were assembled with APS LSM cathode deposited on the densified YSZ to thicknesses of 15, 50, and 100  $\mu\text{m}$ , respectively. The effect of LSM thickness on the output performance of a SOFC single cell is shown in Fig. 7. It can be seen that ohmic polarization was mainly responsible for the reduction of cell voltage when the thickness of the LSM cathode was about 15  $\mu\text{m}$ . However, for the cell assembled with an APS LSM cathode of thickness 50  $\mu\text{m}$  the concentration polarization of the cathode becomes significant at current densities higher than 0.3  $\text{A}/\text{cm}^2$ . This result indicates that the porosity of the APS LSM was not high enough to permit the use of a thick LSM layer. A thick APS LSM layer results in a significant reduction of the maximum output power density. When the thickness of the cathode was increased from 15 to 100  $\mu\text{m}$ , the maximum power density at 1000  $^\circ\text{C}$  decreased from 0.72 to 0.42  $\text{W}/\text{cm}^2$ .

There are large voids, nonbonded lamellar interfaces, and vertical cracks in individual lamellae (Ref 4). A network of microcracks and nonbonded interfaces interconnects voids throughout the coating, which permits reaction gas species to pass through coating. However, the connected porosity of plasma-sprayed ceramic coatings decreases remarkably with increasing coating thickness (Ref 6, 27). In other words, the thicker the APS LSM coating, the more difficult gas transportation through the coating becomes. The gas permeability can be improved by increasing the porosity of the APS LSM deposit, whereby the use of thick APS LSM may become possible. However, the electrical conductivity of APS LSM decreases with increasing porosity. Therefore, further

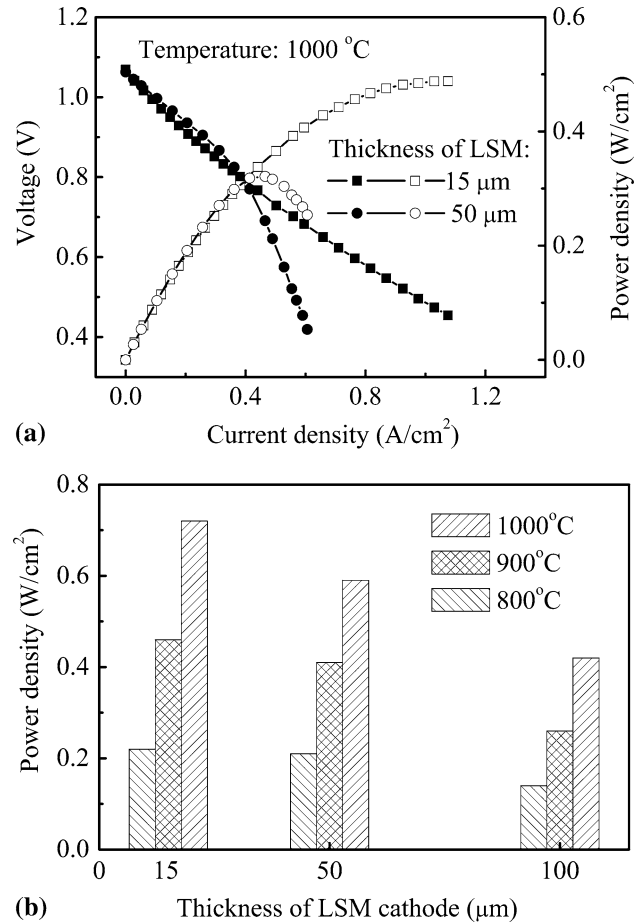


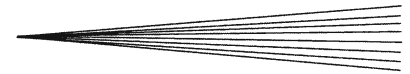
**Fig. 7** Effect of LSM thicknesses on the output performance of SOFC single cells: (a) the output performances of two cells with 75  $\mu\text{m}$  thick YSZ and (b) effect of APS LSM thickness on the maximum power density

improvement of the cathode performance through increasing porosity of the deposit should take into account the electrical conductivity of the APS LSM.

## 4. Summary

Tubular SOFCs have been assembled by thermal-spray techniques. A Ni-Al<sub>2</sub>O<sub>3</sub> supporting tube was deposited by flame spray, and the anode, YSZ electrolyte, and LSM cathode were fabricated by APS. The effects of APS YSZ thickness, APS anode compositions, and APS LSM cathode thickness on the output performance of the SOFC cell were investigated.

A SOFC cell incorporating as-sprayed YSZ as the electrolyte exhibited a low OCV due to its high gas permeability. The gas permeability of APS YSZ can be significantly reduced by one order in magnitude by infiltration treatment of the porous coating using yttrium/zirconium nitrate solutions. SOFC cells assembled with this densified APS YSZ exhibited an OCV approximately



equal to the theoretical value. The result indicates that the densification to APS YSZ electrolyte using the present postspray densification treatment makes it applicable to SOFC.

The performance of a SOFC strongly depends on the APS composite anode microstructure. It can be significantly improved by designing YSZ-NiO composite feedstock powder in such a way as to increase the active TPB length.

The performance of a SOFC is also remarkably influenced by the conductivity and thickness of the APS YSZ electrolyte. It has been found that decreasing the electrolyte thickness and increasing its electrical conductivity led to enhanced performance of the SOFCs. The maximum output power density of about 0.76 W/cm<sup>2</sup> at 1000 °C was obtained when the YSZ electrolyte thickness was reduced to about 40 μm. When APS ScSZ was used as the electrolyte, the maximum output power density was increased to 0.89 W/cm<sup>2</sup> at 1000 °C owing to the higher electrical conductivity of ScSZ compared to that of YSZ. Moreover, it was observed that when a thick APS LSM cathode was employed, concentration polarization of the cathode became significant.

## Acknowledgments

The present project was supported by the National High Technology Research and Development Program of China (Grant no. 2007AA05Z135) and Research and Development of Science and Technology of Shaanxi Province (Grant no. 2006K07-G28)

## References

1. R.A. George, Status of Tubular SOFC Field Unit Demonstrations, *J. Power Sour.*, 2000, **86**, p 134-139
2. S.C. Singhal, Advances in Solid Oxide Fuel Cell Technology, *Solid State Ionics*, 2000, **135**, p 305-313
3. R.A. George and N.F. Bessette, Reducing the Manufacturing Cost of Tubular SOFC Technology, *J. Power Sour.*, 1998, **71**, p 131-137
4. C.-J. Li and A. Ohmori, Relationship Between the Structure and Properties of Thermally Sprayed Coatings, *J. Therm. Spray Technol.*, 2002, **11**(3), p 365-374
5. C.-J. Li, A. Ohmori, and R. McPherson, The Relationship Between Microstructure and Young's Modulus of Thermally Sprayed Ceramic Coatings, *J. Mater. Sci.*, 1997, **32**, p 997-1004
6. A. Ohmori, C.-J. Li, Y. Arata, K. Inoue, and N. Iwamoto, Dependence of the Connected Porosity in Plasma Sprayed Ceramic Coatings on Structure, *J. Jpn. High Temp. Soc.*, 1990, **16**, p 332-340 (in Japanese)
7. M. Fukumoto, K. Negoro, I. Okane, M. Kitoh, and S. Fukami, Fabrication of Solid Oxide Fuel Cell Electrodes by Plasma Spraying of Ni/YSZ Mechanically Alloyed Composite Powders, *J. Jpn. Inst. Metal*, 1994, **58**(1), p 50-54
8. K. Barthel, S. Rambert, and St. Siegmann, Microstructure and Polarization Resistance of Thermally Sprayed Composite Cathodes for Solid Oxide Fuel Cell Use, *J. Therm. Spray Technol.*, 2000, **9**(3), p 343-347
9. L.J.H. Kuo, S.D. Vora, and S.C. Singhal, Plasma Spraying of Lanthanum Chromite Films for Solid Oxide Fuel Cell Interconnection Application, *J. Am. Ceram. Soc.*, 1997, **80**(3), p 589-593
10. K. Okumura, Y. Aihara, S. Ito, and S. Kawasaki, Development of Thermal Spraying-Sintering Technology for Solid Oxide Fuel Cells, *J. Therm. Spray Technol.*, 2000, **9**, p 354-359
11. K.A. Khor, L.G. Yu, S.H. Chan, and X.J. Chen, Densification of Plasma Sprayed YSZ Electrolytes by Spark Plasma Sintering (SPS), *J. Eur. Ceram. Soc.*, 2003, **23**, p 1855-1863
12. C.-J. Li, C.-X. Li, and X.-J. Ning, Performance of YSZ Electrolyte Layer Deposited by Atmospheric Plasma Spraying for Cermet Supported Tubular SOFC, *Vacuum*, 2004, **73**, p 699-703
13. C.-J. Li, X.-J. Ning, and C.-X. Li, Effect of Densification Process on the Properties of Plasma-Sprayed YSZ Electrolyte coatings for Solid Oxide Fuel Cell, *Surf. Coat. Technol.*, 2005, **190**, p 60-64
14. O. Takayasu, K. Yasuo, and M. Akihiko, New Tubular Type SOFC Using Metallic System Components, *Denki Kagaku*, 1996, **64**(6), p 555-561
15. K. Yasumoto, N. Mori, J. Mizusaki, H. Tagawa, and M. Dokiya, Effect of Oxygen Nonstoichiometry on Electrode Activity of La<sub>1-x</sub>A<sub>x</sub>MnO<sub>3</sub> Cathode, *J. Electrochem. Soc.*, 2001, **148**, p A105-A111
16. A.J. Mcevoy, Materials for High-Temperature Oxygen Reduction in Solid Oxide Fuel Cells, *J. Mater. Sci.*, 2001, **36**, p 1087-1096
17. C.-J. Li, C.-X. Li, and M. Wang, Effect of Spray Parameters on the Electrical Conductivity of Plasma-Sprayed La<sub>1-x</sub>Sr<sub>x</sub>MnO<sub>3</sub> Coating for the Cathode of SOFCs, *Surf. Coat. Technol.*, 2005, **198**, p 278-282
18. X.-J. Ning, C.-X. Li, C.-J. Li, and G.-J. Yang, Modification of Microstructure and Electrical Conductivity of Plasma-Sprayed YSZ Deposit Through Post-Densification Process, *Mater. Sci. Eng. A*, 2006, **428**, p 98-105
19. C.-X. Li, X.-J. Ning, and C.-J. Li, Preparation of YSZ Electrolytic Layer for SOFC by Plasma Spraying Combined with Densification Process, *Chin. J. Power Sour.*, 2004, **28**(9), p 565-569 (in Chinese)
20. H. Tsukuda, A. Notomi, and N. Hisatome, Application of Plasma Spraying to Tubular-Type Solid Oxide Fuel Cells Production, *J. Therm. Spray Technol.*, 2000, **9**(3), p 364-368
21. J. Will, A. Mitterdorfer, C. Kleinlogel, D. Perednis, and L.J. Gauckler, Fabrication of Thin Electrolytes for Second-Generation Solid Oxide, *Solid State Ionics*, 2000, **131**, p 79-96
22. M. Lang, R. Henne, S. Schaper, and G. Schiller, Development and Characterization of Vacuum Plasma Sprayed Thin Film Solid Oxide Fuel Cells, *J. Therm. Spray Technol.*, 2001, **10**(4), p 618-625
23. R. Henne, Solid Oxide Fuel Cells: A Challenge for Plasma Deposition Processes, *J. Therm. Spray Technol.*, 2007, **16**(3), p 381-403
24. R. Hui, Z.W. Wang, O. Kesler, L. Rose, J. Jankovic, S. Yick, R. Maric, and D. Ghosha, Thermal Plasma Spraying for SOFCs: Applications, Potential Advantages and Challenges, *J. Power Sour.*, 2007, **170**, p 308-323
25. C.-J. Li, C.-X. Li, Y.-Z. Xing, M. Gao, and G.-J. Yang, Effect of YSZ Electrolyte Thickness on the Characteristics of Plasma-Sprayed Cermet Supported Tubular SOFC, *Solid State Ionics*, 2006, **177**, p 2065-2069
26. C.-J. Li, C.-X. Li, Y.-Z. Xing, Y.-X. Xie, and H.-G. Long, Influence of the Characteristics of Stabilized Zirconia Electrolyte on the Performance of Cermet Supported Tubular SOFCs, *Rare Metals*, 2006, **25**, p 273-279
27. Y. Arata, A. Ohmori, and C.-J. Li, Electrochemical method to evaluate the connected porosity in ceramic coatings, *Thin Solid Films*, 1988, **156**, p 315-325